Prediction of Emission and Performance of a Variable Compression Ratio Engine with Gasoline/Ethanol Blend Using Response Surface Methodology

Palani, Thennarasu
Department of Automobile Engineering, Velammal Engineering College, Chennai, INDIA

Esakkimuthu, Ganapathy Sundaram**+, *Dhamodaran, Gopinath
Department of Mechanical Engineering, Velammal Engineering College, Chennai, INDIA

Seetharaman, Sathyanarayanan
Department of Mechanical Engineering, Easwari Engineering College, Chennai, INDIA

ABSTRACT: *In this study, the effects of ethanol-butanol/gasoline blends (EB0%, EB10%, and EB20%) on spark ignition engine performance and emissions were investigated for the different compression ratios (6.0:1, 8.0:1, and 10.0:1), and different load conditions (2kW, 4kW, and 6kW). Based on the experimental results, the response surface methodology has been used to develop a model and to estimate the outputs of brake thermal efficiency, brake-specific energy consumption, carbon monoxide, hydrocarbon, and oxides of nitrogen. The optimum operating conditions, 9.970% of the ethanol-butanol blend, 10.0:1 compression ratio, and 6 kW of engine load were obtained through the desirability approach of response surface methodology. Brake thermal efficiency, brake-specific energy consumption, carbon monoxide, hydrocarbon, and oxides of nitrogen at optimum conditions are 35.041 %, 0.493 kg/kWh, 0.217 %, 213.575 ppm, and 1263.787 ppm, respectively. Moreover, the developed models have higher R^2 values near 1, and the optimum responses are obtained with a higher desirability value of 0.768. Ethanol-butanol/gasoline blends improved the brake thermal efficiency, carbon monoxide, and hydrocarbons. Whereas it increased the brake-specific energy consumption and oxides of nitrogen. In addition, the validation test results illustrate that the acceptable error rate between the optimized value obtained through the desirability approach of response surface methodology and experimental values is below 7%.*

KEYWORDS: *Oxygenate; spark ignition, carbon monoxide; optimization and response surface methodology.*

INTRODUCTION

The global energy demand and environmental issues are the keys to creating the need for alternate energy sources everywhere [1,2]. In the transport sector, electrical, gaseous, and liquid fuels are the primary energy

**To whom correspondence should be addressed.*
\+ *E-mail: ganapathy_sundar@yahoo.com*
1021-9986/2023/9/3114-3134 21/$/6.01

sources, but liquid fossil fuels have been dominating for more than a century. However, fossil fuels produce dangerous emissions, which affect the environment directly and indirectly. As a result, the environment starts to get damaged [3–6]. Many countries have implemented strict emission norms to reduce the impact of fossil fuel emissions and create an interest in researchers in finding alternate energy sources, especially for the automobile sector [7,8].

Alcohol-based fuels have a long history as alternate fuels to reduce exhaust emissions and improve the performance of internal combustion engines [9]. Besides being a renewable and readily available resource, vegetable oils can also be used as an alternative to fossil fuels, increasing interest. But, these vegetable oil-based alternative fuels are preferably used in diesel engines [10–14]. Extensive research has been carried out on oxygenated alcohols such as methanol, ethanol, and butanol with gasoline and concluded that oxygenated alcohols have the potential to reduce exhaust gas emissions and improve energy efficiencies [15–21]. Alcohol fuels can be used in a near CO_2-neutral manner in engines through efficient biomass conversion, which may be considered an essential renewable solution [22]. Ethanol is the most attractive alcohol fuel to use with gasoline in internal combustion engines due to its favorable properties and its production from renewable sources. Several studies [23–30] have concluded that ethanol-blended gasoline fuel significantly improves torque, mean effective pressure, brake power, brake thermal efficiency, volumetric efficiency, combustion efficiency, cylinder pressure, cylinder temperature, and flame speed.

Elfasakhany [15] researched the five different fuels as ethanol (E), methanol (M), n-butanol (nB), isobutanol (iB), and acetone (AC) blended with gasoline and compared under the same blending rates of 3%, 7% and 10% by volume with gasoline and same engine working conditions to identify the effective blending fuel with gasoline. Results showed that E blends produce maximum power output from the engine, and M blends produce maximum output torque and volumetric efficiency. Also, the nB and iB blends are the worst among all other test fuels. *Thangavel et al.*, [31] investigated ethanol-gasoline and n-butanol-gasoline blends in the PFI SI engine. Two separate injectors are mounted in the intake manifold to inject gasoline and oxygenates separately. The engine operated with ethanol-gasoline produced higher torque and engine efficiency. E30S blend produced 5.2% higher torque and 1% higher efficiency than gasoline. Using 60% of n-butanol by mass with gasoline increases HC emission and reduces the efficiency and torque of the engine because of poor vaporization of n-butanol. The study concluded that the torque and efficiency of the ethanol-gasoline blend are comparatively higher than the n-butanol-gasoline blend. But in recent experimental works, n-butanol has been shown better oxygenate fuel for spark-ignition engines, and also this will be the next generation fuel [32]. Butanol has properties very similar to gasoline and can be blended with gasoline in any blending ratio without any engine modifications. However, many studies have found that butanol improves engine efficiency and reduces exhaust emissions [33–35]. According to the investigations, [36,37] n-butanol has superior properties compared to ethanol, including the ability to blend with gasoline without any restrictions as well as higher energy content. It can also be transported through existing facilities as a blended form without risk of water contamination. In addition, n-butanol has a lower octane number compared to gasoline, which reduces knocking at the higher compression ratio condition. n-butanol has a much lower latent heat of vaporization (582 kJ/kg) than ethanol (904 kJ/kg) and can solve engine cold start and ignition problems. These properties indicate that n-butanol has the potential to overcome the drawbacks of ethanol as an alternate fuel in SI engines [38]. *Fagundez* [39] investigated pure n-butanol and a blend of n-butanol/ethanol as fuels in a spark ignition engine and concluded that n-butanol blends are safe and can be used as fuel, especially with ethanol. [40] found that n-butanol-gasoline blends improve the brake thermal efficiency and reduce peak in-cylinder temperature in SI direct injection gasoline engines. By comparing six different n-butanol-gasoline blends, they concluded that Bu40 (Butanol 40%) is the most suitable fuel. The n-butanol-gasoline blends can reduce CO and NOx emissions but increase HC emissions. Also, [41] introducing ethanol/butanol-gasoline blends at different ratios (0, 2, 5, 10, 15, and 20%) into unmodified engines showed a clear improvement in performance and smooth engine operation under different operating conditions. The CO and HC emissions reduced noticeably as compared to conventional gasoline fuel.

In recent times instead of conducting experiments

Table 1: Fuel Properties [26,37]

S.No	Properties	Ethanol	n-Butanol	Gasoline
1	Molecular formula	C_2H_5OH	C_4H_9OH	C_4-C_{12}
2	Molecular weight	46	74	95-120
3	Oxygen content (wt.%)	34.8	21.5	0
4	Octane number	108	89	>90
5	Density (kg/m^3)	785	810	740
6	Lower heating value (MJ/kg)	26.9	33.1	44.3
7	Latent heat of vaporization (kJ/kg)	840	716	349
8	Boiling temperature (ºC)	78	118	38-204
9	Auto ignition temperature (ºC)	425	343	228-470
10	Stoichiometric AFR	9.0	11.2	14.8

practically, the experiments are simulated with the help of computer applications to reduce the time, cost, and effort for many trials. Response Surface Methodology (RSM) has been a preferred application in recent years. RSM is the statistical method for modeling and analyzing engineering problems influenced by several variables. The goal is to find the relationship between the responses and input variables also to optimize these variables [42,43]. In addition, RSM can develop an analysis of variance (ANOVA) based on the effects of input variables on the outputs [44]. In many experimental studies, RSM has been used to optimize SI engines using alcohol fuels. *Uslu* [45] studied the effects of acetone-gasoline mixture performance and emissions at different speeds and ignition advances on SI engines. Additionally, Artificial Neural Networks (ANN) and RSM models were developed to predict and optimize the results. The optimal operating factors are a 2% acetone ratio, 1700 rpm of speed, and 11º of bTDC. The RSM simulation shows that the R^2 values of all the responses are higher than 0.96, and the obtained desirability value is 0.76523. *Yaman et al*., [46] experimented with three different 1-heptanol percentages, three different compression ratios, and three loads in a PFI spark ignition engine. According to the experiment results, the optimized engine variables found by RSM are 8% 1- heptanol percentage, 10.0:1 CR, and 6 kg engine load. *Yusri et al*., [47] optimized engine performance and emissions of a four-cylinder, four-stroke SI engine using 2-butanol gasoline blended fuel by RSM. The operating conditions are optimal at 3205 rpm, and 15% 2-butanol is blended with gasoline to produce 32.2 kW, 0.66 MPa, 289.3 g/kWh, 29.2% BP, BMEP, BSFC, and BTE. As measured by exhaust emissions, NOx, CO, CO_2, and HC emissions are 858.7 ppm, 1.9%, 5.8%, and 51.3 ppm, respectively. In addition to optimizing SI engines using bio-ethanol fuel blends, *Najafi et al*., [48] investigated the same optimization pattern for engines using bio-ethanol fuel blends. Their optimum engine operating condition is 3000 rpm and 10% bio-ethanol and 90% gasoline blend. Based on exhaust emissions of 3.5% of CO, 12.8% of CO_2, 136.6 ppm of HC, and 1300 ppm of NOx, they generated 35.26 kW of power, 103.52 Nm of torque, and 0.25 kg/kWh of BSFC. *Sathyanarayanan et al*., [49] investigated the effect of diisopropyl ether (DIPE)-gasoline mixtures performance and emission parameters of twin-cylinder SI engine and optimized using RSM. The engine speed, compression ratio, and DIPE fuel blends are input factors, and the optimal values obtained are 2000 rpm, 8 CR, and 25 %, respectively. The selected output responses are BTE, SFC, HC, CO, and NOx, and their predicted optimum values are 31.5332 %, 0.292285 kg/kWh, 31.6701 ppm, 0.138615 %, 708.333 ppm, respectively. *Uslu* and *Celik* [50] investigated optimizing the performance and emissions parameters of an engine fuelled with 1-amyl alcohol/gasoline blends using the ANN-supported RSM model. The optimal operating parameters were 15% i-amyl alcohol, 2957 rpm engine speed, and 8.31 CR. Similar investigations have been conducted by *Simsek* and *Uslu* [51] but using fusel oil and concluded that 30% of fusel oil, 8.39 compression ratio, and 3777-watt engine load are the optimum operating conditions, and the optimized responses are obtained with a higher desirability value of 0.7685. *Abdalla et al*., [52] also examined the fusel oil gasoline blends in SI engines and optimized the parameters with less than 6% error by RSM.

Many studies have been carried out on ethanol- gasoline

Table 2: Fuel blend specifications

Fuel type	Unit	ASTM	EB10	EB20
γ	~	~	0.10	0.20
ρ_f	(kg/m^3)	D1298-99	771	775
h_f	(MJ/kg)	D240	42.59	41.19
ϕ_f	(kg/kg)	~	14.24	13.78
RON		2699	92.15	92.30

Table 3: Test engine specification

S.No.	Description	Specification
1	Make	Kirloskar VCR engine
2	Type	Single cylinder, four stroke
3	Bore (mm)	87.50
4	Stroke (mm)	110.00
5	Connecting Rod length (mm)	234.00
6	Compression ratio	6.0:1 – 10.0:1
7	Swept volume (cc)	661.45
8	Max. Power (kW @ 1800 rpm)	6.5
9	Cooling type	Water cooled

Fig. 1: Photographic view of experimental setup

and butanol-gasoline mixtures as fuel and optimized their operating parameters using Response Surface Methodology (RSM). However, the detailed literature shows no study has been carried out on the optimization of dual oxygenates (ethanol/butanol) - gasoline mixture in spark ignition engine with RSM. In this regard the present study is carried out to enhance the performance of SI engines fueled with an ethanol-butanol-gasoline mixture by optimizing both input and output operating variables using the RSM method.

EXPERIMENTAL SECTION

Ethyl alcohol or ethanol is a colorless, transparent liquid made from sugar by fermentation with yeast, corn, barley, and vegetables. Also, butanol can be produced from biomass, algae, corn, and plant materials that contain cellulose [53]. Table 1. shows the essential properties of ethanol and butanol fuels.

Test fuel

In this experimental study, unleaded gasoline was used as a base fuel. The tests were conducted for different ethanol-butanol fuel blends with gasoline on a volume basis. The proportions are EB0 (100% gasoline), EB10 (10% Ethanol-butanol - 90% gasoline), and EB20 (20% Ethanol-butanol - 80% gasoline), and these fuel blend properties are listed in Table 2.

Experimental setup

The performance and emission characteristics were examined in a single-cylinder, four-stroke water-cooled variable compression ratio engine and a water-cooled eddy current dynamometer loads it. Table 3 shows the specifications of the test engine. The experiment was conducted on three different ethanol-butanol fuel blends ranging from 0% to 20% with gasoline and compression ratios of 6:1, 8:1, and 10:1 at the loading conditions from 2 kW to 6 kW. In-cylinder pressure (CP) concerning Crank Angle (CA) was determined using a pressure transducer, and a CA encoder was fitted in the engine cylinder head and crankshaft, respectively. The actual engine setup is presented in Fig. 1.

Experimental procedure

The experiment was conducted at three different ethanol-butanol percentages with gasoline (EB0, EB10, and EB20), three different compression ratios (6.0:1, 8.0:1, and 10.0:1), and at three different load conditions (2 kW, 4 kW, and 6 kW). Also, all the tests were conducted as per the standard warm-up procedure and draining previous fuel by allowing the engine to run for some time before introducing a new fuel. Test readings are recorded as an average of four times repeated experiment results. Engine brake thermal efficiency and brake-specific fuel consumption were recorded, and HC, CO, and NOx were measured with the help of five gas analyzers. The step-by-step experimental flow chart is presented in Fig. 2.

Error analysis of experimental data

To know the correctness of the experimental result, the uncertainty of the experiment needs to be assessed.

Table 4: Measurement accuracy uncertainty details

S. No	Parameters measured	Range	Instrument Accuracy	Estimated Uncertainty
Performance measuring instruments				
1	Engine Speed (rpm)	0-1850 rpm	±25 rpm	+ 0.5%
2	Crank angle	0-360°	±0.1°	+ 0.5%
3	Pressure	0-350 bar	+ 1 bar	+ 0.4%
4	Temperature	0-1500°C	± 1° C	+ 0.15%
5	Time	0-60s	± 0.2 s	+ 0.25%
Properties measuring instruments				
1	Density	0.60-1.160g/m^3	±0.01 g/m^3	0.12
2	Octane analyzer	0-110 RON	±1	0.1
Emission measuring instrument				
1	CO_2	0-20% vol	± 0.1%	+ 0.25%
2	CO	0-10% vol	± 0.01%	+ 0.25%
3	NOx	0-5000 ppm	± 1	+ 0.2%
4	HC	0-10000 ppm	± 1	+ 0.2%
5	O_2	0-50% vol	± 0.01%	+ 0.1%

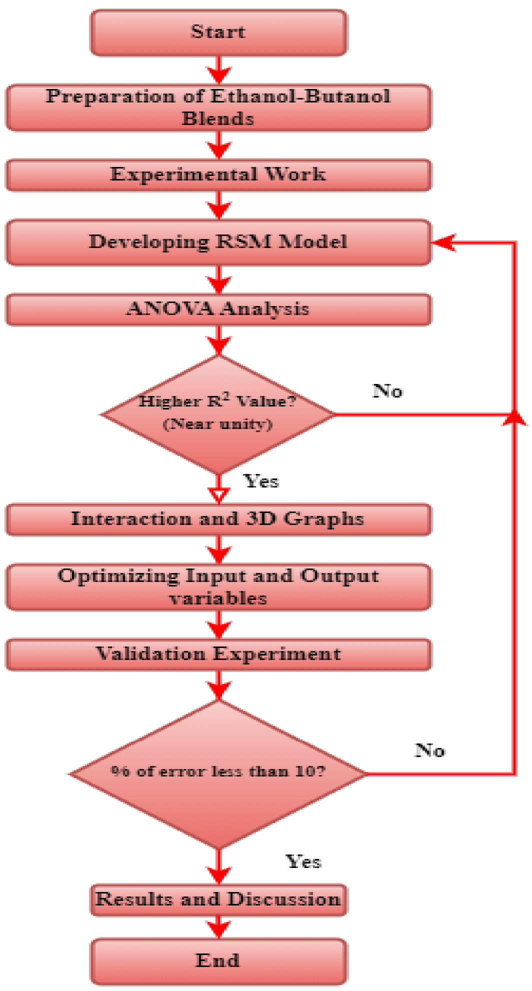

Fig. 2: Experimental flow chart

Uncertainty about the experimental observation arises due to various errors in reading, environment, instrument selection, instrument calibration, working conditions etc. The uncertainty associated with each of the instrument was calculated based on the instrument accuracy as per procedures laid down by *Holman* (2012). The uncertainty percentage of this experiment was calculated using the formula,

$$\left[\sum_{i=1}^{n}(U_{xi})^2\right]^{1/2}$$

Where *Uxi* is the uncertainty associated with each of the measured values using the corresponding instrument. The details of parameters measured and the range of the instrument, the accuracy of the instrument, and % uncertainty associated are listed in Table 4. The calculated uncertainty for performance measurement, properties measuring instrument, and emission instruments are ± 0.654%, ± 0.378 %, and ± 0.463 % respectively. For the complete experiment, the calculated uncertainty is ± 1.495%.

Response surface methodology

RSM is a statistical technique to model and analyses the problems in which the number of variables influences responses, and the aim is to optimize this response [54]. The relationship between dependent and independent factors is unknown in most RSM-based problems. For this reason, the starting stage of RSM is to find the approximate efficient relationship between independent input variables and dependent output variables [55]. The approximation function is the first-order model if a linear relationship is found between input and output factors. The first order polynomial function is expressed in Equation (1) [56].

$$y = \beta_o + \sum_i^k \beta_i x_i + \varepsilon \quad (1)$$

The higher order polynomial can be when model is the second order function [57]

$$y = \beta_o + \sum_i^k \beta_i x_i + \sum_{i=1}^k \sum_{j\geq 1}^k \beta_{ij} x_i x_j + \varepsilon \quad (2)$$

Where y is the predicted response, k is the number of factors, x_i and x_j are independent factors, and ε is the random experimental error or noise. β_o is the constant, β_i is the linear coefficient, β_i j is the interactive coefficient, i is the linear coefficient, and j is the quadratic coefficient. Equation no.3 is used to calculate R^2, equation no.4 is used to calculate adjusted R^2, and Equations (5-7) is used to calculate the predicted R^2 [58].

$$R^2 = 1 - \left[\frac{SS_{residual}}{SS_{residual} + SS_{model}}\right] \quad (3)$$

$$Adj.R^2 = 1 - \left[\frac{\left[\frac{SS_{residual}}{df_{residual}}\right]}{\left[\frac{SS_{residual} + SS_{model}}{df_{residual} + df_{model}}\right]}\right] \quad (4)$$

$$Pred.R^2 = 1 - \left[\frac{PRESS}{SS_{residual} + SS_{model}}\right] \quad (5)$$

$$PRESS = \sum_{i=1}^n (e-1)^2 \quad (6)$$

$$e - 1 = \frac{e_i}{1 - h_{ii}} \quad (7)$$

Where *SS* is the sum of sequential squares, *df* is the degrees of freedom, and *PRESS* is the prediction error sum of squares; *residual* indicates diversityamount, and model indicates how much diversity is explained in the model. *n* is the number of the experimental run, *e* is the response variable, and h_{ii} is the diagonal element of the hat matrix.

Table 5 shows the input variable and the levels chosen for this study. Table 6 shows the optimization setup of input parameters and the importance level for all the responses. In this optimization setup, based on the literature review, authors have chosen fuel blend concentration, CR, and engine load as inputs, and BTE, BSFC, CO, HC, and NOx were considered as outputs. The main objective of this study is to enhance the BTE and reduce the emission level by optimizing the input parameters. Thus, a higher rating importance "5" was given to BTE, CO, and HC. The design matrix was developed using a central composite design in RSM, shown in Table 7. R^2 expresses the relationship between the developed model and experimental results. The R^2 value close to unity indicates that a developed model is significant [59]. Table 8 shows the model assessment, as a result, R^2 values for BTE, BSEC, CO, HC, and NOx were 0.9817, 0.9725, 0.9973, 0.9693, and 0.9966, respectively, showing that the models were highly significant and accurate. Table 9 displays the ANOVA results of the output responses. The higher F and lower p values represent a better degree of significance of the corresponding model. When a p-value is under 0.05, it is considered significant [60]. The predicted p-value for all the models is less than 0.05, which suggests the models were significant with 95% of confidence level [61]. The following are the regression equations obtained for the output responses. Additionally, these equations predict responses based on operating input variables.

BTE = -26.43991 + 0.479527 * EB + 8.87480 * CR + 3.62852 * Load + 0.055625 * EB * CR + 0.025875 * EB * Load - 0.0625000 CR * Load - 0.039886 * EB^2 -0.482159 * CR^2 - 0.138409 * $Load^2$ (8)

BSEC = +2.32332 - 0.028705 * EB - 0.287466 * CR – 0.150670 * Load + 0.002812 * EB * CR – 0.001938 * EB * Load + 0.008437 * CR * Load + 0.001023 * EB^2 + 0.013068 * CR^2 + 0.004318 * $Load^2$ (9)

CO = +1.46777 - 0.016787 * EB - 0.150885 * CR - 0.090498 * Load + 0.000375 * EB * CR + 0.000662 * EB * Load - 0.000438 * CR * Load + 0.000160 * EB^2 + 0.006984 * CR^2 + 0.005634 * $Load^2$ (10)

HC = +99.02273 - 0.123182 * EB + 60.97386 * CR + 3.85568 * Load - 0.556250 * EB * CR + 0.106250 * EB * Load + 0.531250 * CR * Load + 0.075909 * EB^2 - 4.22727 * CR^2 - 2.35227 * $Load^2$ (11)

NOx = +667.29091 + 2.83727 * EB – 135.82455 * CR + 76.27273 * Load + 0.125000 * EB * CR – 1.50000 * EB * Load + 7.75000 * CR * Load + 1.42364 * EB^2 + 10.21591 * CR^2 - 2.28409 * $Load^2$ (12)

Table 5: Input variables with levels

Input Variables	Levels		
Ethanol-Butanol Percentage (%)	0	10	20
Compression Ratio	6:1	8:1	10:1
Load (kW)	2	4	6

Table 6: Optimization setup

Name	Goal	Lower Limit	Upper Limit	Importance
A:Ethanol-Butanol Percentage	is in range	0	20	3
B:Compression Ratio	is in range	6	10	3
C:Load	is in range	2	6	3
BTE	maximize	16.33	34.51	5
BSEC	minimize	0.42	0.97	3
CO	minimize	0.177	0.645	5
HC	minimize	183	320	5
NOx	minimize	451	1647	3

Table 7: Design matrix

Run	Ethanol-Butanol Percentage (%)	Compression Ratio	Load (kW)	BTE (%)	BSEC (g/kWh)	CO (%)	HC (ppm)	NOx (ppm)
1	0	10	6	27.68	0. 52	0.288	258	1154
2	10	8	4	30.95	0.55	0.325	276	863
3	10	8	4	29.54	0.57	0.318	286	888
4	10	8	4	31.12	0.52	0.33	266	850
5	0	8	4	22.47	0.62	0.434	304	735
6	20	10	6	34.12	0.68	0.177	183	1647
7	0	10	2	19.54	0.62	0.487	294	649
8	10	8	6	34.51	0.42	0.264	245	1087
9	10	8	2	24.45	0.75	0.442	291	643
10	20	8	4	29.62	0.72	0.259	266	1298
11	20	6	2	16.33	0.97	0.451	281	1054
12	10	8	4	30.24	0.54	0.32	280	877
13	10	8	4	31.26	0.56	0.332	284	890
14	0	6	2	16.41	0.88	0.645	320	451
15	0	6	6	23.97	0.62	0.457	274	894
16	20	10	2	25.49	0.96	0.319	212	1200
17	20	6	6	27.54	0.58	0.312	245	1315
18	10	10	4	31.48	0.59	0.284	246	1046
19	10	6	4	24.73	0.65	0.4328	275	784
20	10	8	4	29.67	0.58	0.318	270	855

Table 8: Model assessment

Model	BTE	BSEC	CO	HC	NOx
Suggested Model	Quadratic	Quadratic	Quadratic	Quadratic	Quadratic
SD	0.9888	0.0245	0.0075	7.49	22.21
Mean	27.06	0.6450	0.3597	267.80	959.00
R^2	0.9817	0.9852	0.9973	0.9693	0.9966
Adjusted R^2	0.9653	0.9718	0.9949	0.9417	0.9935
Predicted R^2	0.8600	0.9162	0.9870	0.8709	0.9589
Adequate Precision	28.0205	31.1786	90.1492	24.8622	75.5184

Table 9: ANOVA results

Source	BTE		BSEC		CO		HC		NOx	
	F-value	p-value	F-value	p-value	F-value	p-value	F-value	p-value	F-value	p-value
Model	59.66	< 0.0001	73.88	< 0.0001	413.60	< 0.0001	35.10	< 0.0001	321.46	< 0.0001
A-Ethanol-Butanol Percentage	54.24	< 0.0001	70.22	< 0.0001	1126.08	< 0.0001	123.44	< 0.0001	1403.77	< 0.0001
B-Compression Ratio	87.98	< 0.0001	18.10	0.0017	988.02	< 0.0001	72.82	< 0.0001	291.05	< 0.0001
C-Load	212.6	< 0.0001	307.39	< 0.0001	1281.6	< 0.0001	66.47	< 0.0001	894.32	< 0.0001
AB	10.13	0.0098	42.07	< 0.0001	8.06	0.0176	17.67	0.0018	0.1014	0.7567
AC	2.19	0.1696	19.96	0.0012	25.15	0.0005	0.6447	0.4407	14.60	0.0034
BC	0.511	0.4909	15.14	0.0030	0.4387	0.5227	0.6447	0.4407	15.59	0.0027
A^2	44.75	< 0.0001	47.80	< 0.0001	12.66	0.0052	2.83	0.1236	113.03	< 0.0001
B^2	10.46	0.0090	12.49	0.0054	38.43	0.0001	14.03	0.0038	9.31	0.0122
C^2	0.862	0.3750	1.36	0.2700	25.01	0.0005	4.34	0.0637	0.4655	0.5106
Cor Total	534.8		0.4061		0.2084		18261.20		1432000	

RESULTS AND DISCUSSION

The next sections discuss the engine performance, pollutants level and optimization and validation when employing ethanol-butanol/gasoline blends.

Performance characteristics

Brake thermal efficiency

Brake thermal efficiency is the conversion efficiency of the fuel used in the engine, indicating the useful power produced from the chemical energy of the fuel [62,63]. Fig 3 shows the percentage of contribution of operating parameters on BTE, depicting the impact of the parameters. The engine load has the largest impact on BTE at 38.88 %, followed by Compression Ratio (CR) and ethanol-blend percentage (EB %) of 16.08 % and 9.91 %, respectively. The interaction plots show that the engine load significantly affects BTE. Fig. 4 (a) illustrates that the effect of EB % at a lower compression ratio was insignificant, but at a high compression ratio gives a significant effect. Fig 4 (b) & (c) give a clear view of the engine load interaction effect with CR and EB %. Engine load significantly affects both lower and higher ranges of CR and EB %. The BTE is increasing with engine load and CR because of higher in-cylinder temperature and pressure, improving combustion efficiency. Also, a higher compression ratio improves expansion work output, and at high temperatures, the rate of CO_2 formation is increased, thus releasing more energy for the fuel combusted [64]. The relation between BTE with EB %, CR, and load is mentioned in equation 8. Based on this equation, the 3D surface plots of Load, CR, and EB % versus BTE are developed and shown in Fig 5 (a), (b) & (c). The CR and EB % influence BTE marginally, as present in Fig 5 (a), but engine load affects BTE more effectively, as depicted in fig 5 (b) and (c). BTE is highest when the load is between 4 and 6 kW, and the EB percentage is between 10 to 20%. Also, the highest BTE can be observed when the load is between 4 to 6 kW and compression ratio 8 to 10. Compared to EB0, both EB10 and EB20 produce higher BTE due to higher flame velocity, latent heat of vaporization, and oxygen concentration improving combustion efficiency. However, fig 6 shows that EB20 produces slightly lower BTE compared to EE10 at a higher compression ratio condition. The maximum 34.51% BTE was observed at CR8 and 6 kW

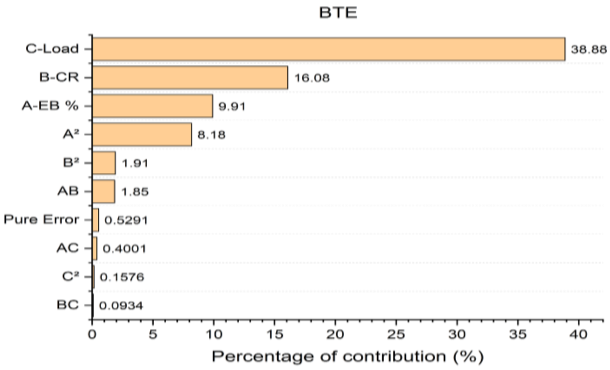

Fig. 3: Percentage of contribution of input factors for BTE

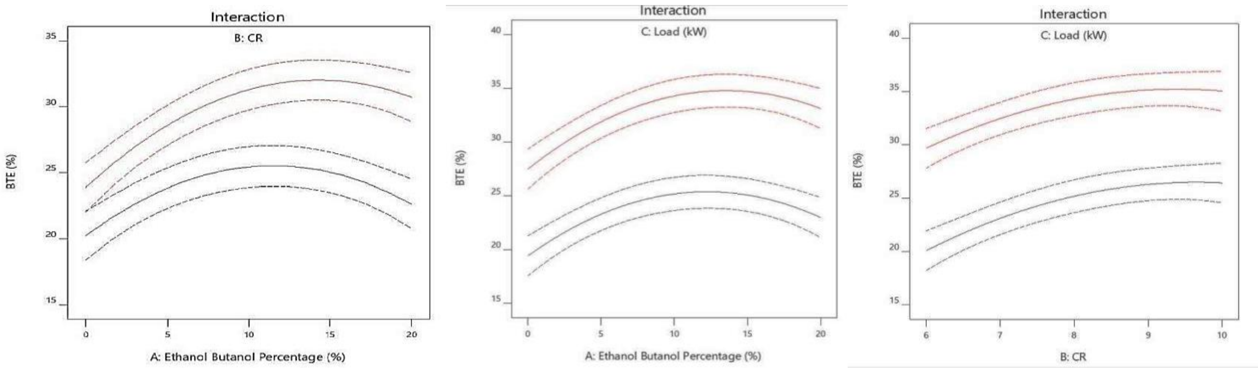

(a) *(b)* *(c)*

Fig. 4: Interaction plot of BTE for (a) Ethanol-Butanol % and CR (b) Ethanol-Butanol % and Load (c) CR and Load

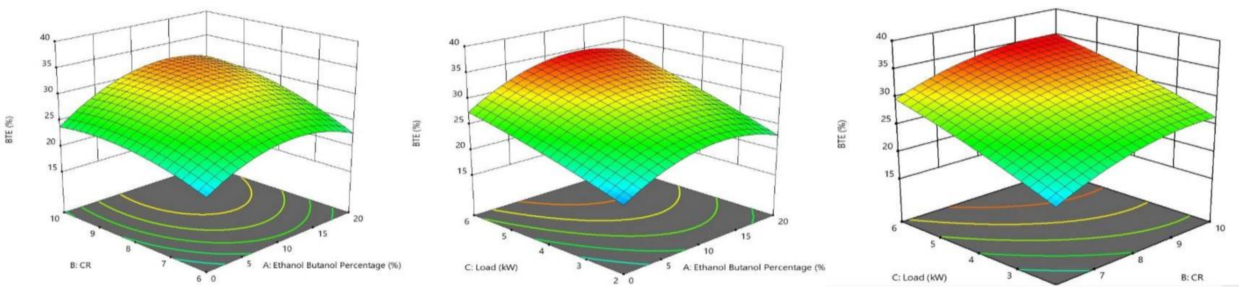

(a) *(b)* *(c)*

Fig. 5: Simultaneous effects of operating variables on BTE (a) CR and Ethanol-Butanol % (b) Load and Ethanol-Butanol % (c) Load and CR

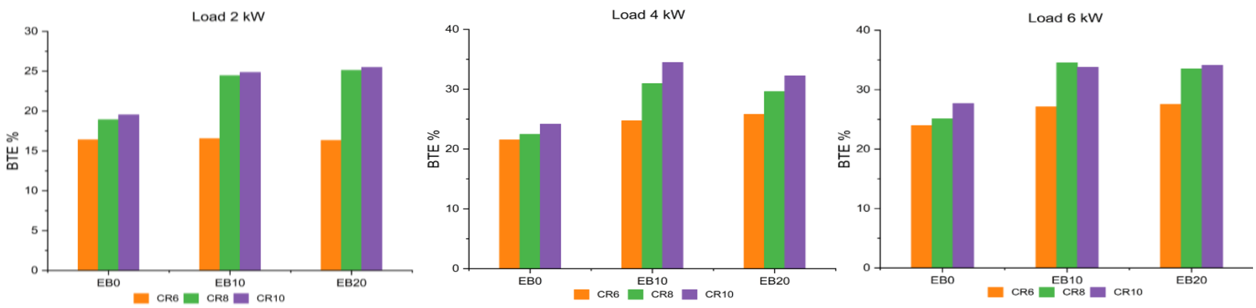

(a) *(b)* *(c)*

Fig. 6: Variation of brake thermal efficiency vs compression ratio (a) 2 kW (b) 4 kW (c) 6 kW

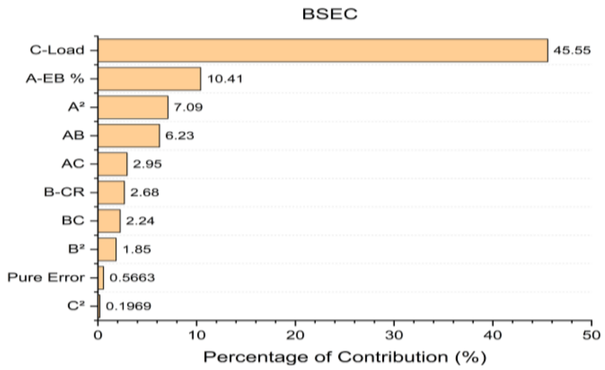

Fig. 7: Percentage of contribution of input factors for BSEC

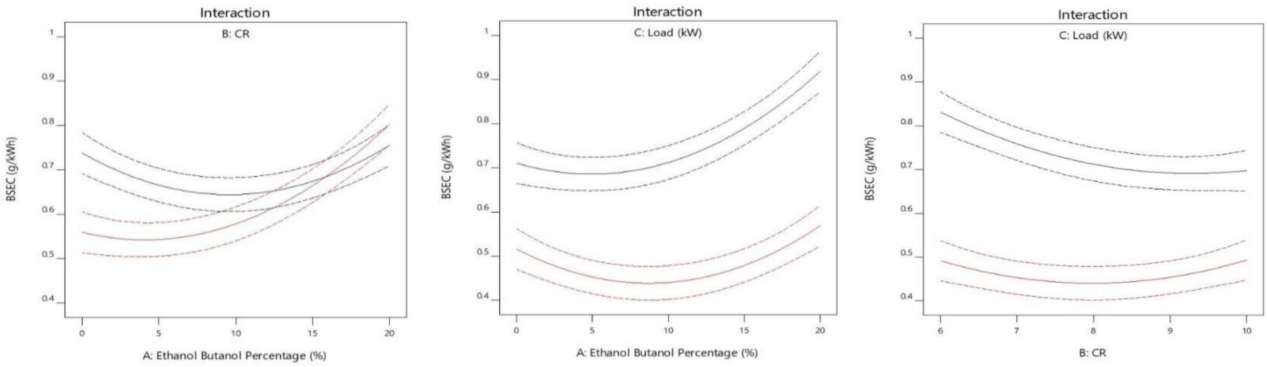

(a) (b) (c)

Fig. 8: Interaction plot of BSEC for (a) Ethanol-Butanol % and CR (b) Ethanol-Butanol % and Load (c) CR and Load

for EB10 fuel, which is 4.76% higher than EB0.

Brake specific energy consumption

Fig. 7 shows the percentage of contribution of operating parameters on BSEC, depicting the impact of the parameters. Among the operating parametrs engine load is the most influincing factors to affect BSEC also EB % affects BSEC moderately and CR perform insignificantly. Fig. 8 shows the interactive effects of the input variables, and fig. 8 (a) displays the interaction between EB% and CR with BSEC. The EB% has an insignificant impact on lower CR, but at high CR significantly affects the BSEC. The increase in fuel consumption at a higher ethanol-butanol percentage is due to the lower calorific value and increased latent heat and burning rate of the fuel. Furthermore, the fuel consumption was reduced at higher CR because of improved in-cylinder pressure and temperature. Fig. 8 (b) & (c) portrays the interactive effect of engine load with CR and EB% on BSEC. Engine load produces a significant impact on BSEC in both lower and higher ranges of CR and EB%. The higher load condition creates higher cylinder pressure and temperature, which will improve the combustion quality and reduces incomplete combustion, resulting in reduced fuel consumption. The combustion temperature for high loads is higher, and the fuel is used more efficiently, resulting in better fuel economy [65]. The relation between BSEC with EB %, CR, and load is mentioned in equation 9. Based on this equation, the 3D surface plots of Load, CR, and EB % versus BSEC are developed and shown in fig. 9 (a), (b) & (c). The peak fuel energy consumption has been observed in the zone of least load condition (2kW) and highest EB% (EB20). Also, the lower fuel consumption was noted in peak load condition and EB10% condition, as indicated in Fig. 9 (b). The variation of BSEC at all the compression ratio and fuel blends are shown in fig. 10. At CR10, 6 kW load, and EB10 operating conditions, the BSEC increased by 5.7% compared to EB0. Still, at the same functional condition, EB20 fuel consumes 30.7% higher BSEC than EB0 because the higher ethanol-butanol percentage affects the overall calorific value of the fuel.

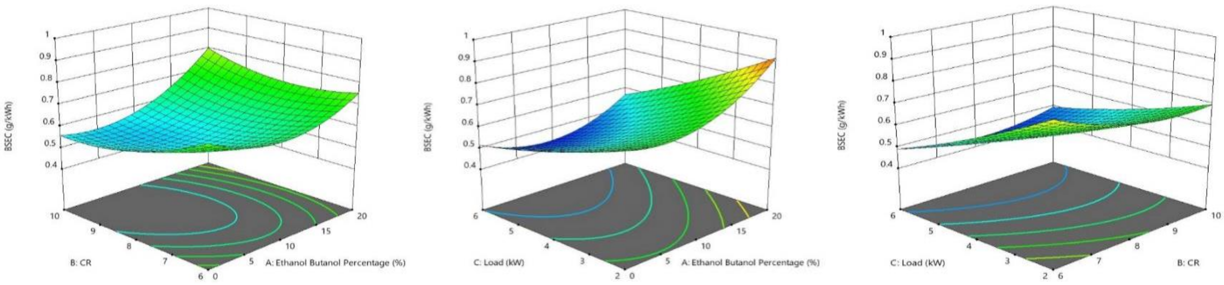

(a) *(b)* *(c)*

Fig. 9: Simultaneous effects of operating variables on BSEC (a) CR and Ethanol-Butanol % (b) Load and Ethanol-Butanol % (c) Load and CR

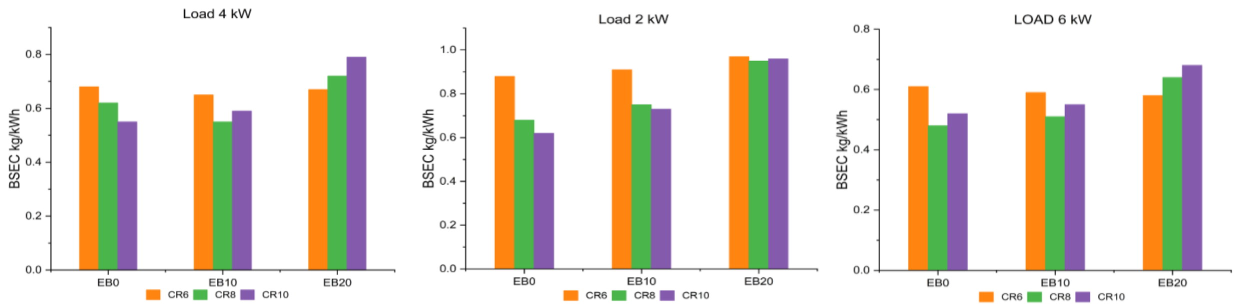

(a) *(b)* *(c)*

Fig. 10: Variation of BSEC vs compression ratio (a) 2 kW (b) 4 kW (c) 6 kW

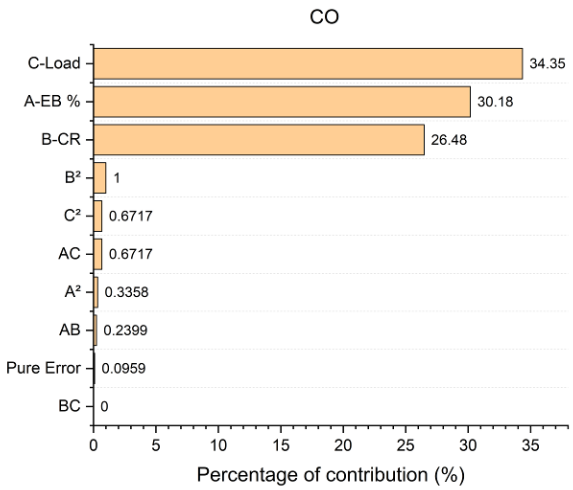

Fig. 11: Percentage of contribution of input factors for CO

Emission characteristics

Carbon monoxide

Carbon monoxide (CO) is the emission produced due to the lack of oxygen in the fuel-air mixture leading to incomplete combustion. Fig. 11 shows the contribution percentage of input variables on the CO emission, presenting that all the input variables significantly affect CO emission. Interactions of input variables with CO are shown in fig. 12. All the interaction curves are in the same trend due to increased load, CR, and EB % reducing CO emission production. Increasing engine load inversely affects CO emission because it increases in-cylinder pressure and temperature, which promotes the conversion of CO into CO_2 rapidly. At the same time, this CO_2 conversion is majorly dependent on the oxygen percentage in the fuel-air mixture. Adding ethanol and butanol in the blended form will produce oxygen enrichment in the fuel and reduce the incomplete combustion of carbon particles. The relation between CO with EB %, CR, and load is mentioned in equation 10. Based on this equation, the 3D surface plots of Load, CR, and EB % versus CO are developed and shown in Fig. 13 (a), (b) & (c) and it has depicted that the lowest CO emission was observed in the higher load, CR, and EB% zone. The CO emission for different CR and loads are represented in fig. 14. Compared with EB0 at CR10, 6 kW load and EB10 fuel reduced CO emissions by 19.1%. Under the same

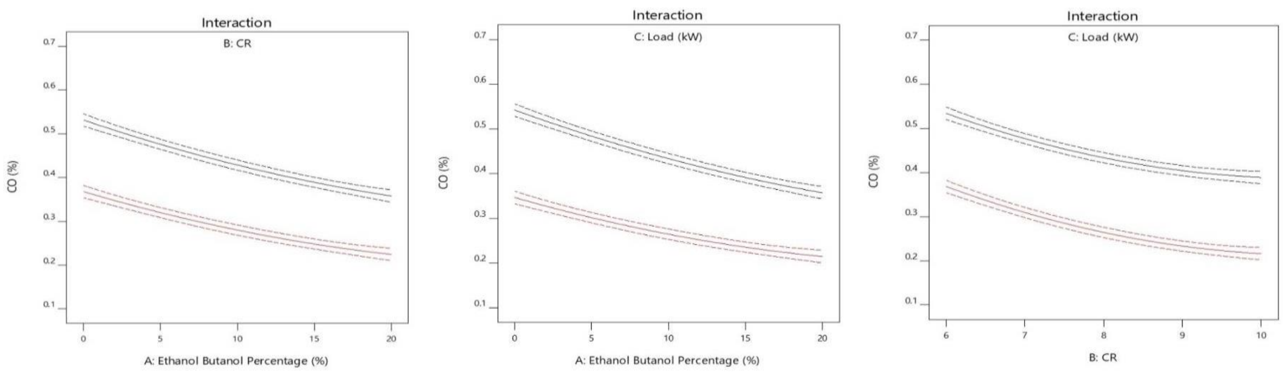

(a) ***(b)*** ***(c)***

Fig.12: Interaction plot of CO for (a) Ethanol-Butanol % and CR (b) Ethanol-Butanol % and Load (c) CR and Load

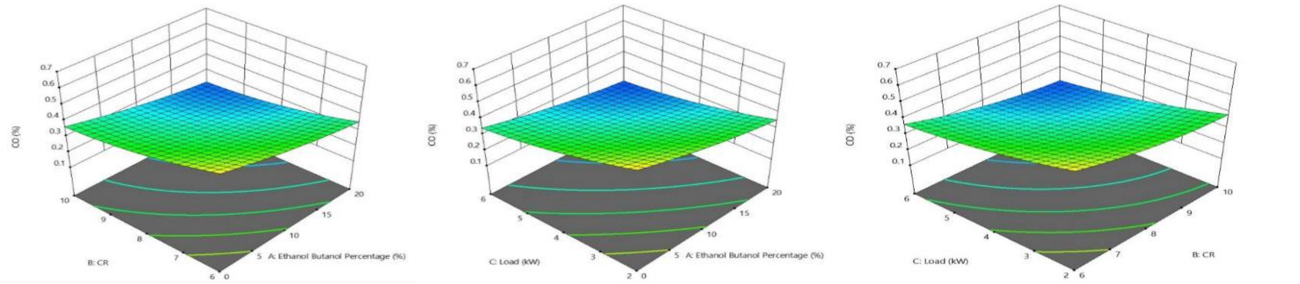

(a) ***(b)*** ***(c)***

Fig.13: Simultaneous effects of operating variables on CO (a)CR and Ethanol-Butanol % (b) Load and Ethanol-Butanol % (c) Load and CR

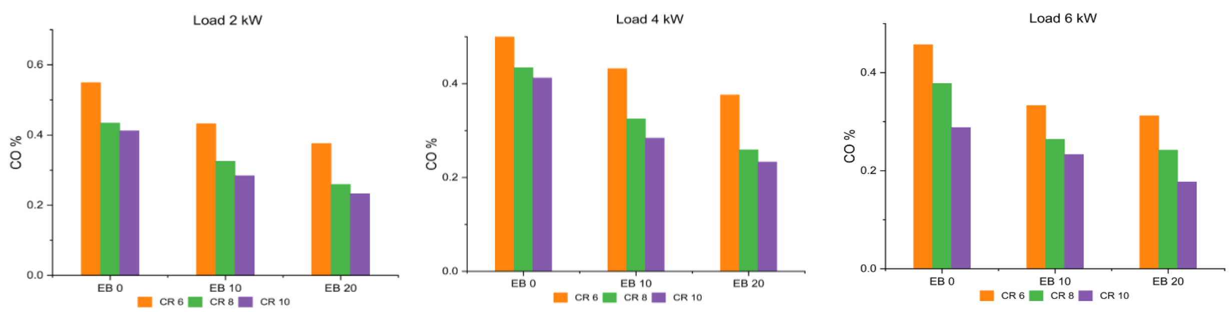

(a) ***(b)*** ***(c)***

Fig.14: Variation of Carbon monoxide vs compression ratio (a) 2 kW (b) 4 kW (c) 6 kW

conditions, CO emissions were observed for EB20 fuel to be a maximum 38.54% reduction than EB0 due to the EB% being the second major impact contributor to CO emission, as represented in fig.11. Higher EB% enhances the conversion efficiency of CO.

Hydrocarbon

Fig. 15 shows the percentage of contribution of input variables on hydrocarbon (HC) emission. EB% has the highest impact with 37.87 % on HC emission, followed by CR and engine load with 22.34% and 20.39%, respectively. The incomplete combustion occurred due to inhomogeneity in the fuel-air mixture, thus producing HC emission in the exhaust. The interaction graphs are presented in fig. 16, and fig. 16 (a) show that at the lower CR condition, the EB% does not affect HC emission significantly, but at the higher CR condition, the reduction of HC emission with increasing EB% was observed most significant effect. Increasing load and CR reduces HC emission drastically, and as depicted in fig. 16 (b) and (c), the interaction between load with CR affects HC emission reduction in the same trend. This HC reduction is due to

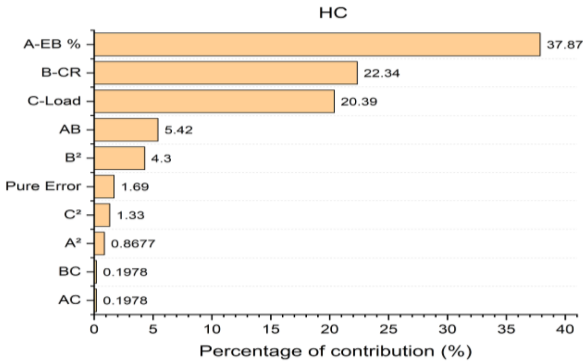

Fig. 15: Percentage of contribution of input factors for HC

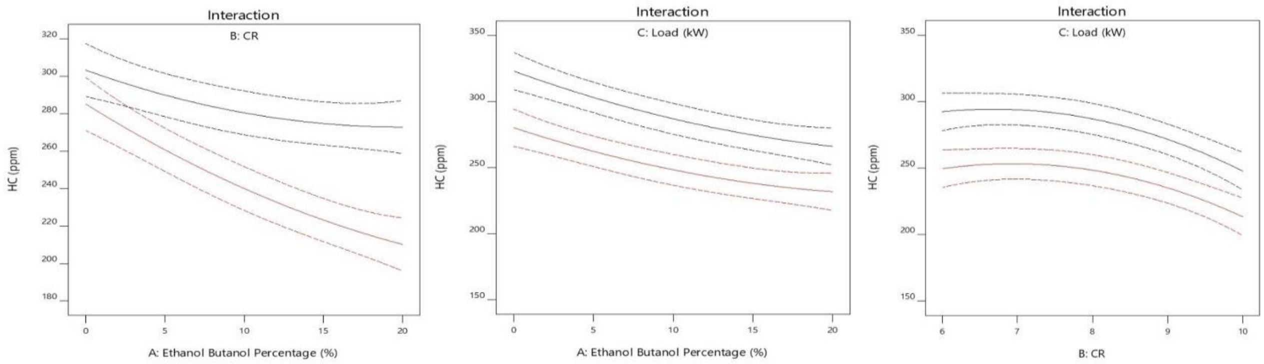

Fig. 16: Interaction plot of HC for (a) Ethanol-Butanol % and CR (b) Ethanol-Butanol % and Load (c) CR and Load

improved combustion temperature and higher oxygen level in the fuel-air mixture, thus promoting complete combustion and reducing incomplete combustion loss. The relation between HC with EB %, CR, and load is mentioned in equation 11. Based on this equation, the 3D surface plots of Load, CR, and EB % versus HC are developed and shown in fig. 17 (a), (b) & (c). The lower HC emission was observed in loads 4 to 6 kW and EB10% to EB20% also at 8 to 10 CR zone. The 19.38% HC emission reduction compared to EB0 was observed at CR10, 6 kW load, and EB10 operating conditions. Furthermore, a maximum of 29.07% of HC emission reduction was noted for EB20 fuel compared to EB0 at the same functional condition. The higher reduction is observed at EB20 because the contribution of EB% is more significant than other operating variables to affect HC emission, as shown in Fig.15. Fig. 18 shows the amount of HC emission present in exhaust emission. The higher EB% increases fuel volatility and increasing CR and load improve flame speed due to higher temperature, resulting in a notable HC emission reduction in the exhaust.

Oxides of nitrogen

Fig. 19 displays the percentage of contribution of input variables NOx emission. EB% contributes more effect on NOx emission with 48.33%, followed by load and CR with 30.79% and 10.02%, respectively. The NOx formation depends on combustion temperature and oxygen content present in the fuel-air mixture [66]. Fig. 20 (a) shows the interaction between CR and EB% on NOx emission. CR has a moderate effect on NOx formation, but EB% substantially impacts NOx because the higher oxygen percentage in the fuel-air mixture promotes NOx formation. Fig. 20 (b) & (c) indicates that engine load and EB% significantly affect NOx emission. Increasing load enhances combustion temperature, which helps dissociation reaction of O_2 in the combustion chamber, as well as this dissociated free oxygen atoms, reach nitrogen molecules and form NOx emissions [67]. The relation between NOx with EB %, CR, and load is mentioned in equation 12. Based on this equation, the 3D surface plots of Load, CR, and EB % versus NOx are developed and shown in Fig. 21 (a), (b) & (c). The highest NOx emission zone was marked in all the graphs (Fig. 21 (a), (b) & (c))

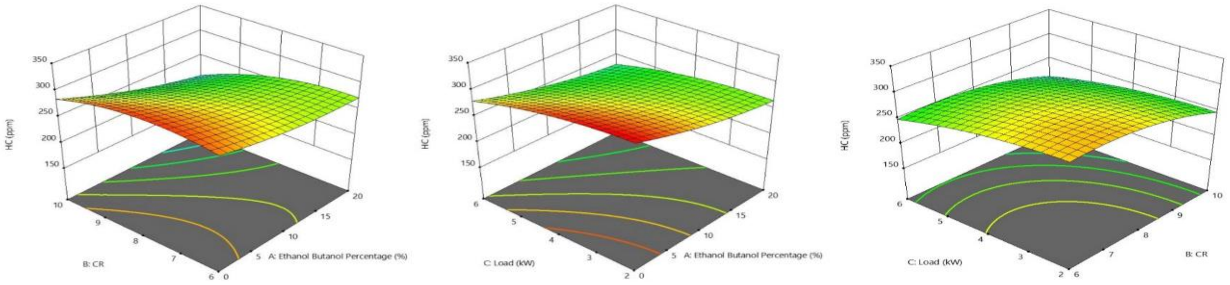

(a) *(b)* *(c)*

Fig. 17: Simultaneous effects of operating variables on HC (a) CR and Ethanol-Butanol % (b) Load and Ethanol-Butanol % (c) Load and CR

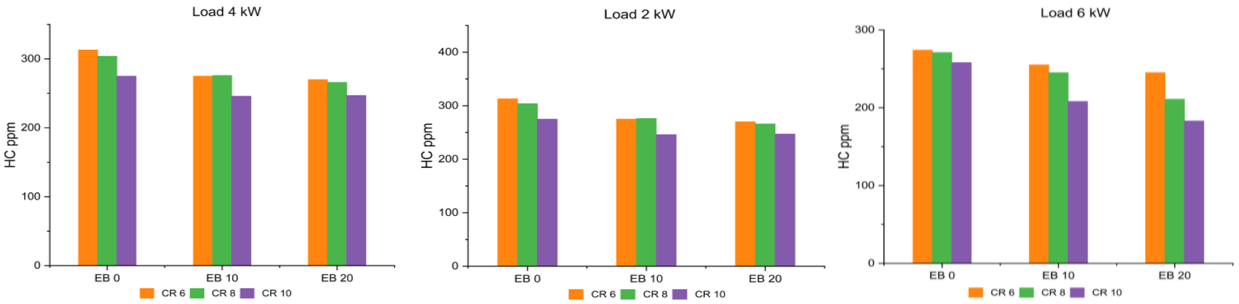

(a) *(b)* *(c)*

Fig. 18: Variation of Hydrocarbon vs compression ratio (a) 2 kW (b) 4 kW (c) 6 kW

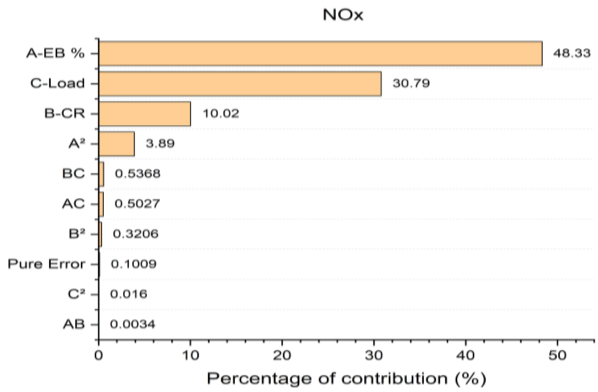

Fig. 19: Percentage of contribution of input factors for NOx

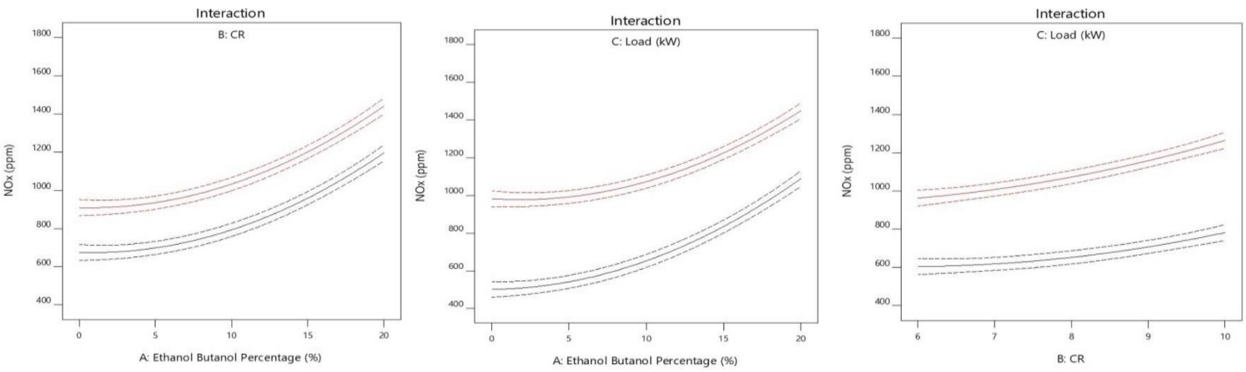

Fig. 20: Interaction plot of NOx for (a) Ethanol-Butanol % and CR (b) Ethanol-Butanol % and Load (c) CR and Load

Table 10: Optimization solutions

Number	Ethanol-Butanol Percentage	Compression Ratio	Load	BTE	BSEC	CO	HC	NOx	Desirability
1	9.970	10.000	6.000	35.041	0.493	0.217	213.575	1263.787	0.768
2	10.027	10.000	6.000	35.063	0.494	0.216	213.379	1265.098	0.768
3	9.885	10.000	6.000	35.007	0.492	0.217	213.884	1261.761	0.768
4	9.870	10.000	6.000	35.000	0.492	0.217	213.934	1261.426	0.768
5	9.922	9.983	6.000	35.031	0.492	0.217	214.179	1260.711	0.768
6	10.049	9.982	6.000	35.082	0.493	0.216	213.769	1263.525	0.768
7	10.160	10.000	5.985	35.091	0.495	0.216	213.170	1266.664	0.768
8	9.891	9.934	6.000	35.046	0.489	0.218	215.554	1254.265	0.768
9	10.161	9.911	6.000	35.162	0.490	0.216	215.178	1258.085	0.768
10	9.670	9.999	5.971	34.872	0.492	0.219	215.207	1253.418	0.767
11	10.005	9.863	6.000	35.125	0.486	0.218	216.917	1248.918	0.767
12	10.755	9.927	6.000	35.363	0.496	0.213	212.740	1274.687	0.767
13	10.333	9.830	6.000	35.262	0.487	0.216	216.632	1252.971	0.767
14	10.260	9.803	6.000	35.246	0.486	0.217	217.544	1248.141	0.767
15	10.222	10.000	5.907	34.987	0.498	0.217	214.342	1259.440	0.766
16	10.085	10.000	5.905	34.932	0.497	0.218	214.861	1255.900	0.766
17	9.308	9.786	6.000	34.873	0.478	0.223	221.230	1224.448	0.766
18	10.083	9.999	5.806	34.768	0.501	0.220	216.596	1244.704	0.765
19	10.806	10.000	5.664	34.783	0.513	0.219	216.425	1247.144	0.762
20	11.087	10.000	5.459	34.510	0.524	0.223	218.712	1231.719	0.758
21	13.792	9.166	6.000	35.948	0.496	0.209	221.636	1284.035	0.751
22	14.632	7.827	6.000	34.457	0.473	0.244	240.770	1198.486	0.725

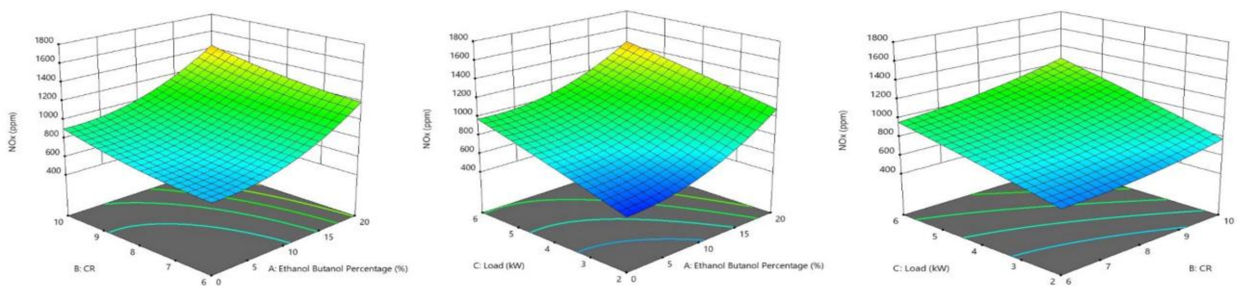

(a) ***(b)*** ***(c)***

Fig. 21: Simultaneous effects of operating variables on NOx (a) CR and Ethanol-Butanol % (b) Load and Ethanol-Butanol % (c) Load and CR

are peak conditions of the input variables because higher load and CR increases combustion temperature and higher EB% increase availability of oxygen concentration results to more reaction between nitrogen and oxygen to form NOx. Fig. 22 shows the NOx emission level present in the exhaust at different EB%, CR, and load conditions. The increasing EB% in gasoline reduces the combustion duration, increases flame velocity, and thus increases flame temperature, resulting in higher NOx formation [68]. The percentage of NOx emission improvement is 15.42% higher than EB0 at CR10, 6 kW load, and EB10 operating conditions. However, at EB20, the obtained maximum NOx emission is 42.72% more than EB0 because of higher CR and EB%.

Optimization and validation test

In this study, the numerical RSM optimization is used

Table 11: Point prediction of engine performance and exhaust gas emission characteristics

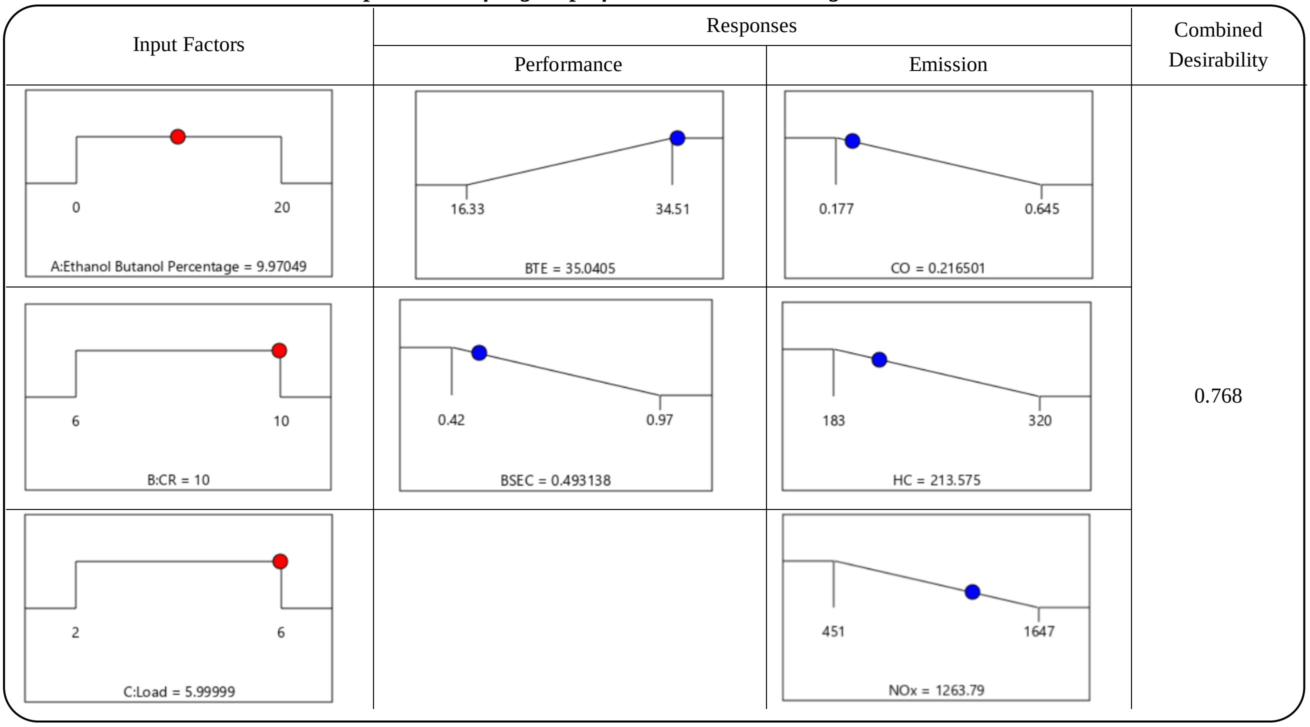

Table 12: Validation test results

	EB (%)	CR	Load (kW)	BTE (%)	BSEC (kg/kWh)	CO (%)	HC (ppm)	NOx (ppm)
Predicted	9.970	10.0:1	6	35.041	0.493	0.217	213.575	1263.787
Actual				33.782	0.468	0.233	208.451	1332
% of Error				3.72	5.34	6.87	2.46	5.12

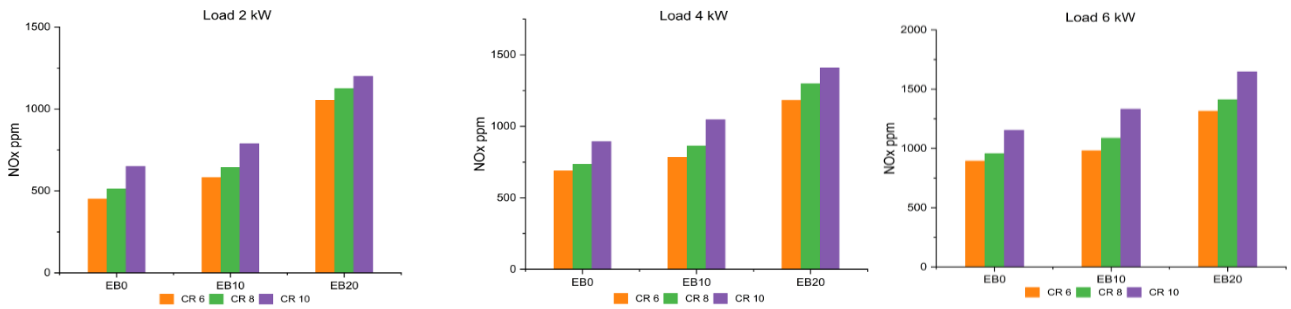

(a) ***(b)*** ***(c)***

Fig. 22: Variation of NOx vs compression ratio (a) 2 kW (b) 4 kW (c) 6 kW

to predict the optimum operating parameters of the engine. Based on the desirability approach, many best solutions were found and listed in the table 10. Solution number 1 was selected for operating parameters with the highest desirability value of 0.768, with the main objectives of maximizing BTE and minimizing BSEC, CO, HC, and NOx. The importance of the responses is assigned from 1 to 5, indicating that they are least to most significant. In this case, the importance of output variables BSEC and NOx are assigned 3 and for remaining variables are 5. According to the optimization results, the optimum input operating conditions are 9.970 EB%, 10.0:1 CR, and 6 kW load. Also, the optimum performance and emission parameters are 35.041% BTE, 0.493 kg/kWh BSEC, 0.217% CO, 213.57ppm HC, and 1263.787 ppm NOx. Table 11 presents the point prediction ramp graphs for all the parameters.

A validation experiment is an essential to verify the accuracy of the optimized operating parameters. The experiment was conducted at 9.970 EB%, 10.0:1 CR, and 6 kW of load condition. The RSM predicted results were validated with the experimental results and tabulated in Table 12. The test engine was configured with the closest RSM predicted optimum parameters, and the output was measured. The error percentage between the experimental results and the RSM results is less than 7%, indicating a good agreement.

CONCLUSIONS

This experiment examines ethanol-butanol blends (0%, 10%, and 20%) on the performance and emission characteristics of variable compression ratio engine at various engine loads (2 kW, 4 kW, and 6 kW) and compression ratios (6.0:1, 8.0:1, and 10.0:1) using RSM to obtain optimum operating conditions. The following results we obtained and summarized below,

- As per ANOVA analysis, all the established models are statistically significant with a 95% confidence level.
- The most optimum operating conditions are obtained by using the desirability approach of RSM. The optimum operating conditions are 9.947% of EB %, 10.0:1 CR, and 6 kW engine load.
- An optimum operating conditions, the performance and emission are 35.041 % BTE, 0.493 kg/kWh BSEC, 0.217 % CO, 213.575 ppm HC, and 1263.787 ppm NOx.
- The maximum BTE was obtained at CR8, 6kW load, and EB10 conditions, which is 4.76% higher than the EB0. All the fuel blends enhanced the BTE at higher CR and load conditions. Adding ethanol-butanol blends improves BTE, CO, and HC but inversely affects BSEC and NOx at higher load and CR.
- The study found that, at CR10, 6 kW load conditions EB20 fuel produced 30.7% higher BSEC as compard to EB0 fuel. Emissions such as CO and HC were reduced notably for all higher CR, load, and blending ratios, and the maximum reduction values are 38.54% and 27.07% higher than EB0, respectively. However, the NOx emission increased at all the higher operating conditions because of enhanced oxygen percentage in fuel.
- The higher R^2 values indicate a higher significance of fit of the model. The adjusted R^2 values for the developed models of BTE, BSEC, CO, HC, and NOx are 0.9653, 0.9718, 0.9949, 0.9417, and 0.9935, respectively.
- The percentage of contribution graphs reveals that the EB % and load significantly affect all the responses.
- The accuracey of results predicted from RSM are validated by the experimental results. The percentage of error between the obtained from RSM and experimental is less than than 7% for all the responses, which shows that the developed models adequately describe the effects of engine performance and emission characteristics.

The results show that ethanol-butanol/gasoline fuel can be used in spark ignition engine to improve BTE and reduce CO and HC emissions. The proposed RSM tool is acceptable and successfully optimized the engine responses according to the input factors chosen. A comparative study of blending single and dual oxygenate with gasoline can be done in the future.

Nomenclature

ANN	artificial neural networks
ANOVA	analysis of variance
BMEP	brake mean effective pressure
BP	brake power
BSEC	brake specific energy consumption
bTDC	before top dead center
BTE	brake thermal efficiency
CA	crank angle
CO	carbon monoxide
CO_2	carbon dioxide
CP	in-cylinder pressure
CR	compression ratio
EB	ethanol-butanol
EB0	pure gasoline
EB10	10% ethanol-butanol – 90% gasoline
EB20	20% ethanol-butanol – 80% gasoline
HC	hydrocarbon
h_f	calorific value of fuel blend
NO	nitrogen oxide
NOx	oxides of nitrogen
O_2	oxygen
ppm	parts per million
R^2	correlation coefficient
RON	research octane number
RPM	revolution per minute
RSM	response surface methodology
γ	volume fraction of oxygenate
ρ_f	density of fuel blend
ϕ_f	stoichiometric air-fuel ratio of fuel blend

Received : Oct. 22, 2022 ; Accepted : Jan. 30, 2023

REFERENCES

[1] Rajakrishnamoorthy P., Karthikeyan D., Saravanan C.G., Emission Reduction Technique Applied in SI Engines Exhaust by Using Zsm5 Zeolite as Catalysts Synthesized from Coal Fly Ash, Mater Today Proc., **22**: 499–506 (2020).

[2] Yusoff M.N.A.M., Zulkifli N.W.M., Masjuki H.H., Harith M.H., Syahir A.Z., Khuong L.S., et al., Comparative Assessment of Ethanol and Isobutanol Addition in Gasoline on Engine Performance and Exhaust Emissions, *J Clean Prod.*,**190**: 483–95 (2018).

[3] Abdellatief T.M.M., Ershov M.A., Kapustin V.M., Chernysheva E.A., Savelenko V.D., Salameh T., et al., Uniqueness Technique for Introducing High Octane Environmental Gasoline Using Renewable Oxygenates and its Formulation on Fuzzy Modeling, *Science of the Total Environment*, **802**: 149863 (2022).

[4] al Shebli M.N., Raj A., Elkadi M., Anjum D., Pena G.D.J., Prabhu A., Fuel Oxygenation as a Novel Method to Reduce Sooting Propensity of Fuels: An Investigation with Gasoline Surrogate Fuels, *Fuel*, **324**: 124562 (2022).

[5] Dhamodaran G., Sundaram Esakkimuthu G., Palani T., Krishnan R., feasibility of Adding Fusel Oil as an Oxygenate to Gasoline on Reducing MPFI Engine Emissions, *Environmental Engineering and Management Journa*l, **21**: 1255-1264 (2022).

[6] Nourozi N., Ebadi A.Gh., Bozorgian A.R., Hoseyni S.J.; Vessally E., Energy and Exergy Analysis of Internal Combustion Engine Performance of Spark Ignition for Gasoline, Methane, and Hydrogen Fuels, *Iran. J. Chem. Chem. Eng. (IJCCE)*, **40(6)**: 1909-1930 (2021).

[7] Chen Z., Zhang Y., Wei X., Zhang Q., Wu Z., Liu J., Thermodynamic Process and Performance of High n-Butanol/Gasoline Blends Fired in a GDI Production Engine Running Wide-Open Throttle (WOT), *Energy Convers Manag.*, **152**:57–64 (2017).

[8] Dhamodaran G, Esakkimuthu GS, Experimental Measurement of Physico-Chemical Properties of Oxygenate (DIPE) Blended Gasoline, *Measurement (Lond).*, **134**: 280–5 (2019).

[9] Bae C, Kim J, Alternative Fuels for Internal Combustion Engines, *Proceedings of the Combustion Institute*, **36**: 3389–413 (2017).

[10] Chidambaranathan B., Kumarasami D.P., Soundararajan G., Thulasiram R., Performance and environmental Impact Assessment of Diesel Engine Operating on High Viscous Punnai Oil–Diesel Blends, *Environmental Science and Pollution Research* (2022).

[11] Bibin C., Devan P.K., Senthil Kumar S., Madhu S., Sheeja R., Characterization of Nonedible Punnai Oil Biodiesel Derived by Two-Stage Transesterification, *Green Energy and Technology.* **1**: 205–29 (2022).

[12] Kumar V.N. G.K., Kutti Y.P., Study on Combustion, Emission and Performance Behaviour of Diesel Engine Using CME Blends, *International Journal of Applied Engineering Research*, **10**: 9017-9031 (2015).

[13] Devan P.K., Chidambaranathan B., Soundararajan G., Ramakrishnan C. , Improvisation of Combustion Behaviour of Jojoba Oil Diesel Blend Fuelled Di Diesel Engine by Engine Modifications Such as Mop and TBC, *Iran. J. Chem. Chem. Eng. (IJCCE)*., **41(7):** 2417-2427 (2022).

[14] D.G., Sundaram E.G., Experimental Studies on Performance and Emission Characteristics of Diesel Engine Fuelled with Neem Oil Methyl Ester Blends, *International Energy Journal*, **15**: 33-42 (2015).

[15] Elfasakhany A., Investigations on Performance and Pollutant Emissions of Spark-Ignition Engines Fueled with n-Butanol–, Isobutanol–, Ethanol–, Methanol–, and Acetone–Gasoline Blends: A Comparative Study, *Renewable and Sustainable Energy Reviews*, **71** :404–413 (2017).

[16] Elfasakhany A., Exhaust Emissions and Performance of Ternary Iso-Butanol–Bio-Methanol–Gasoline and n-Butanol–Bio-Ethanol–Gasoline Fuel Blends in Spark-Ignition Engines: Assessment and Comparison, *Energy*, 1**58**: 830–844 (2018).

[17] Li Y., Meng L., Nithyanandan K., Lee T.H., Lin Y., Lee C Fon F., et al. Combustion, Performance and Emissions Characteristics of a Spark-Ignition Engine Fueled with Isopropanol-n-Butanol-Ethanol and Gasoline Blends, *Fuel*, **184**: 864–872 (2016).

[18] Li Y., Gong J., Deng Y., Yuan W., Fu J., Zhang B., Experimental Comparative Study on Combustion, Performance and Emissions Characteristics of Methanol, Ethanol and Butanol in a Spark Ignition Engine, *Appl. Therm. Eng.*,**115**: 53–63 (2017).

[19] Schifter I., González U., Díaz L., Sánchez-Reyna G., Mejía-Centeno I., González-Macías C., Comparison of Performance and Emissions for Gasoline-Oxygenated Blends up to 20 Percent Oxygen and Implications for Combustion on a Spark-Ignited Engine, *Fuel*, **208**: 673–681 (2017).

[20] Wang Z., Liu H., Reitz R.D., Knocking Combustion In Spark-Ignition Engines, *Prog. Energy Combust. Sci.*, **61**: 78–112 (2017).

[21] Zhen X., Wang Y., Liu D., Bio-Butanol as a New Generation of Clean Alternative Fuel for SI (Spark Ignition) and CI (Compression Ignition) Engines, *Renew Energy*, **147**: 2494–521 (2020).

[22] Awad O.I., Ali O.M., Mamat R., Abdullah A.A., Najafi G., Kamarulzaman M.K., et al. Using fusel Oil as a Blend in Gasoline to Improve SI Engine Efficiencies: A Comprehensive Review, *Renewable and Sustainable Energy Reviews*, **69**: 1232–42 (2017).

[23] Akansu S.O., Tangöz S., Kahraman N., İlhak M.İ., Açıkgöz S., Experimental Study of Gasoline-Ethanol-Hydrogen Blends Combustion in an SI Engine, *Int. J. Hydrogen Energy*, **42**: 25781–25790 (2017).

[24] Altın İ., Bilgin A., Sezer İ., Theoretical Investigation on Combustion Characteristics of Ethanol-Fueled Dual-Plug SI Engine, *Fuel*, **257**: 116068 (2019).

[25] Badra J., AlRamadan A.S., Sarathy S.M., Optimization of the Octane Response of Gasoline/Ethanol Blends, *Appl. Energy*, **203**: 778–93 (2017).

[26] Elfasakhany A., Investigations on the Effects of Ethanol–Methanol–Gasoline Blends in a Spark-Ignition Engine: Performance and Emissions Analysis, *Engineering Science and Technology, An International Journal*, **18**: 713–719 (2015).

[27] Li Y., Duan X., Liu Y., Liu J., Guo G., Tang Y., Experimental Investigation the Impacts of Injection Strategies Coupled with Gasoline/Ethanol Blend on Combustion, Performance and Emissions Characteristics of a GDI Spark-Ignition Engine, *Fuel*, **256**: 115910 (2019).

[28] Sakthivel P., Subramanian K.A., Mathai R., Comparative Studies on Combustion, Performance and Emission Characteristics of a Two-Wheeler with Gasoline and 30% Ethanol-Gasoline Blend Using Chassis Dynamometer, *Appl. Therm. Eng.*, **146**: 726–737 (2019).

[29] Thakur A.K., Kaviti A.K., Mehra R., Mer K.K.S., Progress in Performance Analysis of Ethanol-Gasoline Blends on SI Engine, *Renewable and Sustainable Energy Reviews*, **69**: 324–340 (2017).

[30] Zhuang Y., Zhu G., Gong Z., Wang C., Huang Y., Experimental and Numerical Investigation of Performance of an Ethanol-Gasoline Dual-Injection Engine, *Energy*, **186**: 115835 (2019).

[31] Thangavel V., Momula S.Y., Gosala D.B., Asvathanarayanan R., Experimental Studies on Simultaneous Injection of Ethanol-Gasoline and N-Butanol-Gasoline in the Intake Port of a Four Stroke SI Engine, *Renewable Energy*, **91**: 347–360 (2016).

[32] Guo Z, Yu X, Dong W, Sun P, Shi W, Du Y, et al. Research on the Combustion and Emissions of an SI Engine with Acetone-butanol-Ethanol (ABE) Port Injection Plus Gasoline Direct Injection, *Fuel*, **267**: 117311 (2020).

[33] Guo Z., Yu X., Du Y., Wang T., Comparative Study on Combustion and Emissions of SI Engine with Gasoline Port Injection Plus Acetone-Butanol-Ethanol (ABE), Isopropanol-Butanol-Ethanol (IBE) or Butanol Direct Injection, *Fuel*, **316**: 123363 (2022).

[34] Liu W., Safdari Shadloo M., Tlili I., Maleki A., Bach Q.V., The Effect of Alcohol–Gasoline Fuel Blends on the Engines' Performances and Emissions, *Fuel*, **276**: 117977 (2020).

[35] Yousif I.E., Saleh A.M., Butanol-Gasoline Blends Impact on Performance and Exhaust Emissions of a Four Stroke Spark Ignition Engine, *Case Studies in Thermal Engineering*, **41**: 102612 (2023).

[36] Dhamodaran G., Esakkimuthu G.S., Palani T., Feasibility of Adding N-Butanol and Di Isopropyl Ether with Gasoline on its Physico-Chemical Properties, *Pet Sci Technol.*, **40**: 486–503 (2022).

[37] Dhamodaran G., Esakkimuthu G.S., Pochareddy Y.K., Sivasubramanian H., Investigation of n-Butanol as Fuel in a Four-Cylinder MPFI SI Engine, *Energy*, **125**: 726–735 (2017).

38] Wei H., Feng D., Pan M., Pan J.Y., Rao X.K., Gao D., Experimental Investigation on the Knocking Combustion Characteristics of n-Butanol Gasoline Blends in a DISI Engine, *Applied Energy*, **175**: 346–355 (2016).

[39] Fagundez J.L.S., Golke D., Martins M.E.S., Salau N.P.G., An Investigation on Performance and Combustion Characteristics of Pure N-Butanol and a Blend of n-Butanol/Ethanol as Fuels in a Spark Ignition Engine, *Energy*, **176**: 521–530 (2019).

[40] Tian Z., Zhen X., Wang Y., Liu D., Li X., Combustion and Emission Characteristics of n-Butanol-Gasoline Blends in SI Direct Injection Gasoline Engine, *Renewable Energy*, **146**: 267–279 (2020).

[41] Mourad M., Mahmoud K., Investigation into SI Engine Performance Characteristics and Emissions Fuelled with Ethanol/Butanol-Gasoline Blends, *Renewable Energy*, **143**: 762–771 (2019).

[42] Elkelawy M., el Shenawy E.A., Alm-Eldin Bastawissi H., Shams M.M., Panchal H., A Comprehensive Review on the Effects of Diesel/Biofuel Blends with Nanofluid Additives on Compression Ignition Engine by Response Surface Methodology, *Energy Conversion and Management: X*, **14**: 100177 (2022).

[43] Singh Y., Sharma A., Kumar Singh G., Singla A., Kumar Singh N., Optimization of Performance and Emission Parameters of Direct Injection Diesel Engine Fuelled with Pongamia Methyl Esters-Response Surface Methodology Approach, *Ind. Crops Prod.*, **126**: 218–226 (2018).

[44] Kadir Yesilyurt M., Uslu S., "Response Surface Methodology Based Optimization of a Diesel Engine Fueled with Diethyl Ether/Diesel Fuel Blends", *3rd International Congress of Academic Research, Bolu, Turkey*, **July 20-22** (2020).

[45] Uslu S., Yesilyurt M.K., Yaman H., Impact Prediction Model of Acetone at Various Ignition Advance by Artificial Neural Network and Response Surface Methodology Techniques for Spark Ignition Engine, *Science and Technology for Energy Transition (STET)*, **77**: 7 (2022).

[46] Yaman H., Yesilyurt M.K., Uslu S., Simultaneous Optimization of Multiple Engine Parameters of a 1-Heptanol / Gasoline Fuel Blends Operated a Port-Fuel Injection Spark-Ignition Engine Using Response Surface Methodology Approach, *Energy*, **238**: 122019 (2022).

[47] Yusri I.M., Mamat R., Azmi W.H., Omar A.I., Obed M.A., Shaiful A.I.M., Application of Response Surface Methodology in Optimization of Performance and Exhaust Emissions of Secondary Butyl Alcohol-Gasoline Blends in SI Engine, *Energy Convers Manag.*, **133**: 178–195 (2017).

[48] Najafi G., Ghobadian B., Yusaf T., Ardebili S.M.S., Mamat R., Optimization of Performance and Exhaust Emission Parameters of a SI (Spark Ignition) Engine with Gasolineeethanol Blended Fuels Using Response Surface Methodology, *Energy*, **90**: 1815–1829 (2015).

[49] Sathyanarayanan S., Suresh S., Saravanan C.G., Vikneswaran M., Dhamodaran G., Sonthalia A., et al. Experimental Investigation and Performance Prediction of Gasoline Engine Operating Parameters Fueled with Diisopropyl Ether-Gasoline Blends: Response Surface Methodology Based Optimization, *J. Clean Prod.*, **375**: 133941 (2022).

[50] Uslu S., Celik M.B., Performance and Exhaust Emission Prediction of a SI Engine Fueled with I-amyl Alcohol-Gasoline Blends: An ANN Coupled RSM Based Optimization, *Fuel*, **265**: 116922 (2020).

[51] Simsek S., Uslu S., Experimental Study of the Performance and Emissions Characteristics of Fusel Oil/Gasoline Blends in Spark Ignited Engine Using Response Surface Methodology, *Fuel*, **277**: 118182 (2020).

[52] Abdalla A.N., Tao H., Bagaber S.A., Ali O.M., Kamil M., Ma X., et al. Prediction of Emissions and Performance of a Gasoline Engine Running with Fusel Oil–Gasoline blends Using Response Surface Methodology, *Fuel*, **253**: 1–14 (2019).

[53] Yusri I.M., Mamat R., Najafi G., Razman A., Awad O.I., Azmi W.H., et al. Alcohol Based Automotive Fuels from First four Alcohol Family in Compression and Spark Ignition Engine: A Review on Engine Performance and Exhaust Emissions, *Renewable and Sustainable Energy Reviews*, **77**: 169–181 (2017).

[54] Montgomery D.C., Design and Analysis of Experiments.

[55] Deepanraj B., Senthilkumar N., Ranjitha J, Jayaraj S, Ong HC. Biogas from Food Waste through Anaerobic Digestion: Optimization with Response Surface Methodology, *Biomass Convers Biorefin.*, **11**: 227–239 (2021).

[56] Uslu S., Optimization Of Diesel Engine Operating Parameters Fueled With Palm Oil-Diesel Blend: Comparative Evaluation between Response Surface Methodology (RSM) and Artificial Neural Network (ANN), *Fuel*, **276**: 117990 (2020).

[57] Sathyanarayanan S., Suresh S., Uslu S., Shivaranjani R.S., Chandramohan V.P., Simsek S., Optimization of Gasoline Engine Emission Parameters Employing Commercial and Sucrolite-Catalyst Coated Converter Using Response Surface Methodology, *Int. J. Environ. Sci. Technol.*, (2022)

[58] Simsek S., Uslu S., Simsek H., Proportional Impact Prediction Model of Animal Waste Fat-Derived Biodiesel by ANN and RSM Technique for Diesel Engine, *Energy*, **239**: 122389 (2022).

[59] Sivakumar D.B., Arulmozhi M., Sathyanarayanan S., Sridharan M., Optimization of Gasoline Engine Operating Parameters Fueled with DIPE-Gasoline Blend: Comparative Evaluation Between Response Surface methodology and Fuzzy Logic Expert System, *Process Safety and Environmental Protection*, **158**: 291–307 (2022).

[60] Singh A., Sinha S., Kumar Choudhary A., Author C., Optimization of Operating Parameters of Diesel Engine Powered with Jatropha Oil Diesel Blend by Employing Response Surface Methodology, *International Journal of Renewable Energy Research*, **11**: 2 (2021).

[61] Simsek S., Uslu S., Simsek H., Response Surface Methodology-Based Parameter Optimization of Single-Cylinder Diesel Engine Fueled with Graphene Oxide Dosed Sesame Oil/Diesel Fuel Blend, *Energy and AI*, **10**: 100200 (2022).

[62] Barboza A.B.V., Mohan S., Dinesha P., Influence of Hydrogen Peroxide Emulsification with Gasoline on the Emissions and Performance in an MPFI Engine, *Int J Hydrogen Energy*, **47**: 25034-25043 (2022).

[63] Behçet R., Yakin A., Evaluation of Hydrogen-Containing NaBH4 and Oxygen-Containing Alcohols (CH3OH, C2H5OH) as Fuel Additives in a Gasoline Engine, *Int J Hydrogen Energy*, **47**: 22316–22327 (2022).

[64] Thomas R., Sreesankaran M., Jaidi J., Paul D.M., Manjunath P., Experimental Evaluation of the Effect of Compression ratio on Performance and Emission of SI Engine Fuelled with Gasoline and N-Butanol Blend at Different Loads, *Perspect Sci.*, **8** :743–746 (2016).

[65] Chidambaranathan B., Kumarasami D.P., Raghavan S., Sundaram M., Thermal and Chemical Exhaust Gas Recirculation Potential of Punnai Oil Biodiesel-Fuelled Diesel Engine for Environmental Sustainability, *Environmental Science and Pollution Research*, (2022).

[66] İlhak M.İ., Akansu S.O., Kahraman N., Ünalan S., Experimental Study on an SI Engine Fuelled by Gasoline/Acetylene Mixtures, *Energy*, **151**: 707–714 (2018).

[67] Sivasubramanian H., Effect of Ignition Delay (ID) on Performance, Emission and Combustion Characteristics of 2-Methyl Furan-Unleaded Gasoline Blends in a MPFI SI Engine, *Alexandria Engineering Journal*, **57**: 499–507 (2018).

[68] Sathyanarayanan S., Suresh S., Sridharan M., Effect of Sucrose Catalyst in the Catalytic Converter on Performance and Emission of Spark Ignition Engine, *J. Therm. Sci. Eng. Appl.*, **14 (4)**: 041015 (2021).